Carbohydrate Polymers 99 (2014) 116–125

Contents lists available at ScienceDirect

Carbohydrate Polymers

journal homepage: www.elsevier.com/locate/carbpol

Effect of β-cyclodextrin on the molecular properties of myricetin upon nano-encapsulation: Insight from optical spectroscopy and quantum chemical studies

Sandipan Chakraborty[a], Soumalee Basu[b,1], Soumen Basak[c,*]

[a] Saroj Mohan Institute of Technology, Guptipara, Hooghly 712512, India
[b] School of Biotechnology & Biological Sciences, West Bengal University of Technology, BF-142, Bidhannagar, Kolkata 700064, India
[c] Chemical Sciences Division, Saha Institute of Nuclear Physics, 1/AF Bidhannagar, Kolkata 700064, India

ARTICLE INFO

Article history:
Received 5 May 2013
Received in revised form 10 July 2013
Accepted 4 August 2013
Available online 13 August 2013

Keywords:
Myricetin
β-CD
Steady-state and time-resolved fluorescence spectroscopy
Induced circular dichroism
Dual emission
Antioxidant potency
Quantum chemical calculations

ABSTRACT

Myricetin, a bioactive plant flavonol, readily forms inclusion complex with the drug delivery vehicle beta-cyclodextrin (β-CD). Appearance of typical "dual emission", consisting of normal (470 nm) and ESIPT tautomer (530 nm) bands, with concomitant rise in fluorescence intensity and dramatically blue shifted normal fluorescence of myricetin with increasing β-CD concentration, indicates facile entry of myricetin into the cavity of β-CD. The stoichiometry of the inclusion complex has been established to be equimolar (1:1), with an equilibrium constant of $439 \pm 18\ M^{-1}$ at 25 °C. The driving force of inclusion is attributed to strong van der Waals interaction and formation of hydrogen bond between host (β-CD) and guest (myricetin). Both experimental and theoretical studies indicate that myricetin possibly incorporates within β-CD through its benzoyl moiety. Inclusion in β-CD increases the antioxidant potency of myricetin which has been attributed to the less delocalised HOMO and reduced HOMO–LUMO energy gap in the confined state.

1. Introduction

Flavonoids are polyphenolic plant secondary metabolites that are commonly found in fruits, vegetables, grains, tea, wine, etc. (Middleton, 1998), having broad-spectrum pharmacological and medicinal properties like anti-inflammatory, anti-allergic, anti-viral, anti-bacterial and anti-tumour activities (Lamson & Brignall, 2000; Meijer & van der Sluijs, 1989). Research on flavonoids received impetus with the discovery of the French paradox, i.e., the low cardiovascular mortality rate was observed in Mediterranean populations which were then attributed to their high red wine intake. This effect, at least in part, was attributed to the flavonoids present in red wine (Formica & Regelson, 1995; Groot & Rauen, 1998). Due to their abundance in dietary products and their potential health beneficial and nutritional effects along with low systemic toxicity, flavonoids are of considerable interest for drug development as well as health food supplements.

Myricetin (3,5,7,3′,4′,5′-hexahydroxyflavone; see Scheme 1A), a widely distributed biologically active plant flavonoid, is a strong antioxidant with various therapeutic potential and is used as an anti-carcinogenic, anti-inflammatory, anti-atherosclerotic and anti-thrombotic agent (Ong & Khoo, 1997). It is one of the most potent inhibitors of MMP-2 enzyme activity in COLO 205 cells (Ko, Shen, Lee, & Chen, 2005) and the growth of Gram-positive and Gram-negative bacterial species (Xu et al., 2001). Myricetin has also been shown to inhibit BACE1 (Chakraborty, Kumar, & Basu, 2011; Shimmyo, Kihara, Akaike, Niidome, & Sugimoto, 2008) which, along with its strong ability to destabilise preformed Aβ fibrils and dose dependent inhibition of fibril growth (Ono et al., 2003), further extends the applicability of myricetin as a therapeutically important compound in Alzheimer's disease. But the applicability of such flavonoids as drugs is often hindered by their low aqueous solubility and in vivo enzymatic degradation, which seriously limits their bioavailability. Encapsulation into suitable delivery vehicles has been suggested as a method to overcome their lack of bioavailability. Cyclodextrins (CDs), which are cyclic oligomers of α-D-glucose units connected to form doughnut shaped truncated cones, are extensively used as additives to increase the solubility of poorly water-soluble organic compounds by the formation of an inclusion complex (Chaudhuri, Chakraborty, & Sengupta, 2010;

* Corresponding author. Tel.: +91 33 2337 5345; fax: +91 33 2337 4637.
E-mail address: soumen.basak@saha.ac.in (S. Basak).
[1] Present address: Department of Microbiology, University of Calcutta, 35 Ballygunge Circular Road, Kolkata 700019, India.

0144-8617/$ – see front matter © 2013 Elsevier Ltd. All rights reserved.
http://dx.doi.org/10.1016/j.carbpol.2013.08.008

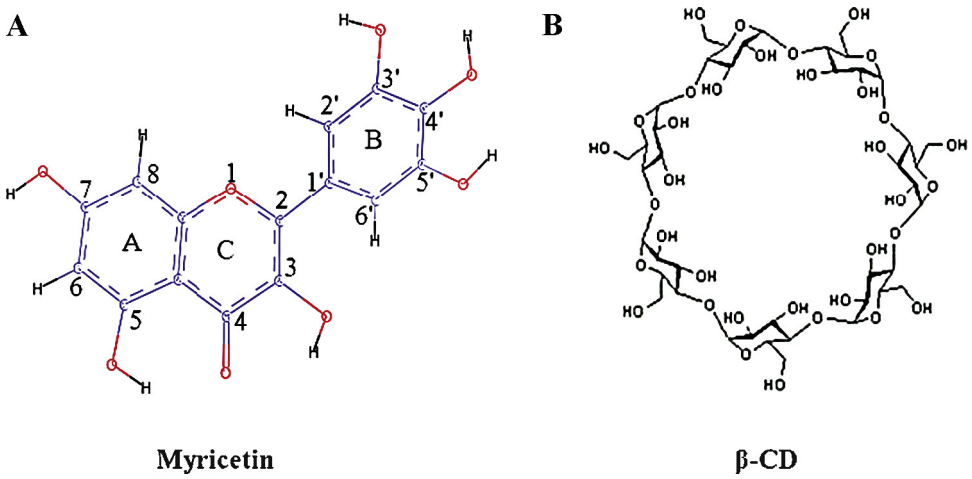

Scheme 1. Structure of (A) myricetin and (B) β-CD.

Kusumoto, 1987; Loftsson, Másson, & Sigurdsson, 2002; Miyake et al., 2000; Paul & Guchhait, 2010; Rusa, Luca, & Tonelli, 2001; Soujanya, Krishna, & Samanta, 1992). Such non-covalent associations can improve the guest's water solubility, bioavailability, and stability. For example, in a recent work using phase-solubility study it was demonstrated that encapsulation in β-CD enhances the solubility of myricetin three times compared to aqueous solution (Kwon, Kim, Park, & Jung, 2010).

The structure of β-CD is depicted in Scheme 1B. Recently, it was shown that β-CDs inhibit the enzymatic oxidation of quercetin and myricetin in acidic medium by horseradish peroxidase in presence of H_2O_2 (Lucas-Abellán, Fortea, Gabaldón, & Núñez-Delicado, 2007). Currently, more than forty approved drugs based on CDx inclusion complexes are available in the market (Rasheed, Kumar, & Sravanthi, 2008). Inclusion in the CDx cavity increases their rate of dissolution and the solubility limit (frequently by a factor of 10^1–10^3), which ultimately leads to a reduction of T_{max} (time to reach the blood level peak after administration of the drug) with a concomitant increase of C_{max} (the attained highest blood level concentration of the drug), two most important pharmacokinetic aspects of drugs (Szejtli, 2004).

CDs have a hydrophobic cavity of diameter 0.45–0.8 nm, while their external surface is highly polar due to presence of several hydroxyl groups in their primary and secondary hydroxyl rim (Rasheed et al., 2008; Szejtli, 2004). This marked difference in polarity should influence the molecular properties of the encapsulated compounds. In a recent study we have demonstrated that a related flavonoid, chrysin, readily incorporates into β-CD cavity and upon inclusion its antioxidant potency increases due to destabilisation of HOMO (Chakraborty, Basu, Lahiri, & Basak, 2010). This result opens up a new aspect of CDx chemistry, wherein CDs are not only used to improve the pharmacokinetic aspects but also can significantly modulate the activity of the included compound, specifically those properties that are related to the electron distribution of the encapsulated compound, i.e., antioxidant activity.

The aim of the present work is to understand the effect on the molecular and electronic properties of myricetin upon its nano-encapsulation in β-CD. The photophysics of encapsulated myricetin has been studied by both steady-state and time-resolved fluorescence spectroscopy by exploiting the intrinsic dual emission behaviour of myricetin. Effect of β-CD on the chirality of encapsulated myricetin has also been addressed by induced circular dichroism spectroscopy (ICD). The present study, for the first time, provides insights regarding the mode of inclusion of myricetin in the β-CD nanocavity through detailed analysis of the energetics involved in the host–guest inclusion process by combining optical spectroscopy with molecular modelling and quantum chemical calculations. The last named have been employed to gain a detailed understanding of the molecular mechanism of enhancement of bioactive properties of myricetin upon inclusion in the β-CD nanocavity.

2. Materials and methods

2.1. Materials

Myricetin and β-CD were purchased from Sigma–Aldrich (99% pure according to the manufacturer). 2,2-Diphenyl-2-picrylhydrazyl (DPPH) was also purchased from Sigma–Aldrich. All solvents employed in spectrophotometric analyses were of analytical grade (E. Merck) and were checked for absence of absorbing impurities. Deionised water from a Milli-Q system apparatus (Millipore Corp., Billerica, MA) was used throughout the experiments.

2.2. Methods

2.2.1. Absorption and fluorescence spectroscopic measurements

Concentrated stock solutions of 1 mM myricetin in ethanol and 12 mM β-CD in Milli-Q water were prepared by vortexing. β-CD solutions of different concentrations were then prepared by diluting the stock. Aliquots from the myricetin stock solution were transferred into specific volumes of β-CD solution to obtain a final concentration of 10 μM myricetin. Samples were equilibrated at room temperature for 1 h before being used for spectroscopic measurements. UV-visible absorption spectroscopy was carried out using a Unicam UV 500 spectrophotometer. Steady state fluorescence measurements were performed at 25 °C on a Jovin-Yvon Fluoromax 3 spectrofluorometer equipped with a Peltier temperature-controller, using a quartz cuvette of path length 1 cm. Fluorescence titration of myricetin with β-CD was carried out at three different temperatures (25 °C, 30 °C and 35 °C) using the temperature-controller. Fluorescence anisotropy (r) values were calculated using the expression

$$r = \frac{I_{VV} - GI_{VH}}{I_{VV} + 2GI_{VH}} \quad (1)$$

where I_{VV} and I_{VH} are the vertically and horizontally polarised components of emission, respectively, with excitation by vertically polarised light and $G\,(=I_{HV}/I_{HH})$ is the sensitivity factor of the detection system (Lakowicz, 1999).

Excited state lifetimes of myricetin were measured on a time-resolved fluorescence spectrometer (FLUOROCUBE, Horiba

Jovin-Yvon) operated in the time-correlated-single-photon-counting (TCSPC) mode using a pulsed LED (pulse width < 1 ns) emitting at 377 nm as the excitation source. Fluorescence intensity decay curves were fitted to a sum of exponentially decaying functions given by:

$$I(t) = \sum_i \alpha_i \exp\left(-t/\tau_i\right), \quad (2)$$

where $I(t)$ is the fluorescence intensity at time t and α_i is a factor representing the fractional contribution to the time-resolved decay of the component with a lifetime of τ_i. The fitting was performed using an iterative routine based on the Marquardt algorithm imbedded in the Decay Analysis Software (version 6.4) provided by Horiba Jobin Yvon. Reduced χ^2-value and the Durbin–Watson (DW) Parameter served as indicators of goodness of fit. The average lifetime $\langle\tau\rangle$ is defined by:

$$\langle\tau\rangle = \frac{\sum_i \alpha_i \cdot \tau_i^2}{\sum_i \alpha_i \cdot \tau_i} \quad (3)$$

2.2.2. Induced circular dichroism

Circular dichroism (CD) spectra were obtained from a Jasco J-720 spectropolarimeter, using a cylindrical quartz cuvette of path length 1 mm. Three successive spectra were measured and averaged for each sample, using a bandwidth of 1.0 nm and a scan speed of 50 nm/min. Induced CD spectra shown were obtained by subtracting the spectra of only β-CD from those of myricetin + β-CD mixtures. Myricetin concentrations were varied from 20 to 80 μM while β-CD concentration was kept constant at 10 mM. All measurements were done at ambient temperature (298 K).

2.2.3. Anti-oxidant activity analysis by DPPH radical scavenging assay

The method is based on the ability of antioxidant molecules to scavenge the long-lived DPPH radical, which has a characteristic absorption at ~517 nm. Addition of antioxidants to the preformed radical reduces it to DPPH, which does not possess that characteristic absorbance, leading to decrease of its absorbance at 517 nm (Burits & Bucar, 2000). A stable stock solution of DPPH was prepared in ethanolic media. Aliquots from this were added to myricetin alone in solution as well as to myricetin together with varying concentrations of β-CD. The final concentration of DPPH in reaction mixture was 75 μM, while that of myricetin was kept at 1 μM. Mixtures were shaken and kept in the dark for 30 min. Three independent measurements of the radical absorbance at 517 nm were recorded using a Varian Cary 100 spectrophotometer at ambient temperature. The effect of β-CD on the antioxidant ability of encapsulated myricetin was nullified by subtracting the effect of β-CD on DPPH absorbance.

The percentage reduction of DPPH absorbance ($I\%$) with respect to ethanol as blank was taken as a measure of free radical scavenging activity:

$$I\% = \left[\frac{A_{\text{Control}} - A_{\text{Sample}}}{A_{\text{Control}}}\right] \times 100 \quad (4)$$

where A_{Control} is the absorbance of DPPH (dissolved in ethanol) and A_{Sample} is the absorbance of DPPH in presence of myricetin and increasing concentration of β-CD.

2.2.4. Molecular docking

Structure of myricetin was built using HYPERCHEM (Hyperchem, 2002) molecular builder and geometry minimised using a semi-empirical method (AM1) to a root-mean square (RMS) gradient of 0.01 kcal/Å mol with Polak–Ribiere conjugate gradient algorithm, implemented in the HYPERCHEM 8.0 package. The β-cyclodextrin structure was extracted from the crystal structure of β-CD complex obtained from Protein Data Bank (PDB ID 3CGT). β-CD was also geometry minimised using AM1 method to an RMS gradient of 0.01 kcal $Å^{-1}$ mol^{-1} with Polak–Ribiere conjugate gradient algorithm. Both the optimised structures were used as a starting structure in the docking study. Structures of both myricetin and β-CD were then prepared for docking in AutoDock (version 4.0) (Morris et al., 1998). AutoDock4 with Lamarckian Genetic Algorithm (LGA) was used for docking study. An initial population of 150 individuals with a maximum number of energy evaluations of 2,500,000 and a maximal number of generations of 27,000 were used as an end criterion. An elitism value of one was used and a probability of mutation and crossing-over of 0.02 and 0.8 was used, respectively. We have defined the conformational search space implementing an $80 \times 80 \times 80$ grid and 0.375 Å spacing between each point in such a way that it covered both the external surface and the internal cavity of the β-CD. A total of 250 docking runs were carried out. At the end of each run, the solutions were separated into clusters according to their lowest RMSD and the best energy score value based on an empirical free energy function. Clustering was performed on the docked complexes with a cut-off of 2 Å.

2.2.5. Conformational search and quantum chemical calculations

We observed mainly two different modes of inclusion of myricetin within β-CD cavity during docking simulations. These are inclusion through the A (chromone) ring and the B (phenyl) ring. For both types of inclusion complex, we started with docked structures generated during the docking process. Structures were fully minimised using Polak–Ribiere conjugate gradient with an RMS gradient of 0.001 kcal $Å^{-1}$ mol^{-1} by using the semi-empirical method PM3 implemented in HYPERCHEM 8.0. Wave functions were further optimised using Density Functional Theory (DFT) using two different basis sets (3-21G* and 6-31G) with B3LYP functional as implemented in GAMESS (Schmidt et al., 1993). Solvent effects were modelled using polarisable continuum model (PCM).

3. Results and discussion

3.1. Electronic absorption & fluorescence spectra

Fig. 1 shows the fluorescence emission profile and absorption spectra (inset) of myricetin in presence of varying concentrations of β-CD. The UV-absorption spectrum of flavonoids is characterised by two principal absorption bands, Band I (340–380 nm) and Band II (240–285 nm). Band I is attributed to light absorption by the cinnamoylic portion (B + C ring) of the molecule whereas Band II arises from its benzoyl moiety (A + C ring). Both these bands are believed to be essentially π–π^* in nature (Zeng, Yang, Liu, & Tang, 2003). For myricetin in aqueous medium, Band I appears at 367 nm. On addition of β-CD, a slight bathochromic shift to 370 nm occurs with an attendant increase in the intensity. This change indicates an interaction between myricetin and β-CD and formation of ground-state complex. The small change in magnitude indicates that the β-CD cavity is not sufficiently large to incorporate the entire molecule, and the immediate micro-environment of the cinnamoylic portion (B + C) of myricetin is only slightly perturbed in presence of β-CD.

The fluorescence spectrum of myricetin in aqueous solution consists of a broad single band, which can be attributed to the strong overlap between its normal and tautomer emissions. However, the intensity of this emission is very low, this being the result of interference of intra-molecular hydrogen bonding present in myricetin along C(4)═O···HO—(5)C co-ordinate. ESIPT occurs along the internal hydrogen bond C(4)═O···HO—(3)C (Sengupta & Kasha, 1979), while the other hydrogen bond C(4)═O···HO—(5)C

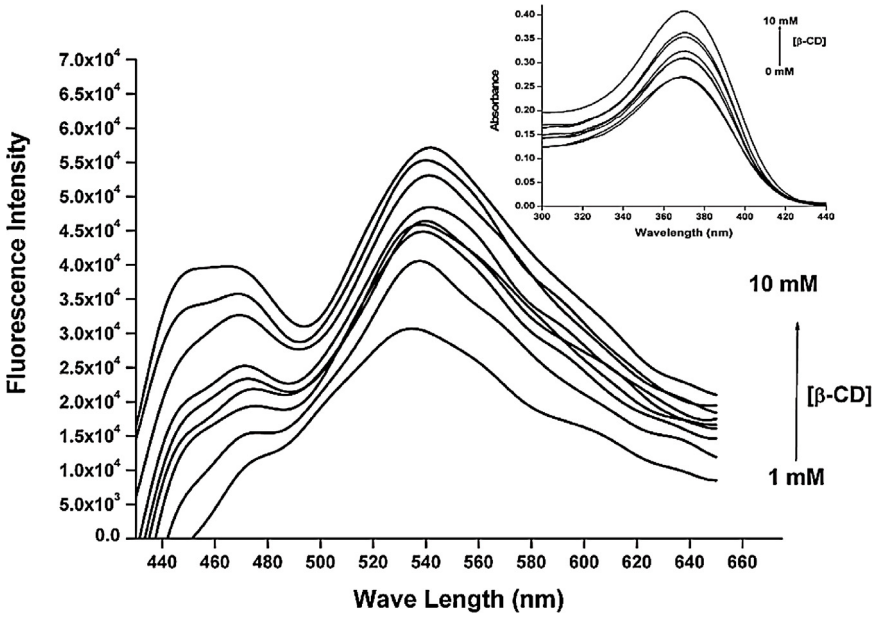

Fig. 1. Fluorescence emission spectra of myricetin (λ_{ex} = 370 nm) in presence of various concentrations of β-CD. Inset displays the absorption spectra of myricetin in presence of various concentrations of β-CD.

facilitates the deactivation process, thus perturbing the ESIPT process. This explains the very low quantum yield of myricetin in aqueous solution. Upon addition of β-CD, typical dual fluorescence emission behaviour of myricetin appears, consisting of normal (blue, 470 nm) and ESIPT tautomer (green, 530 nm) bands with concomitant rise in the fluorescence intensity, suggesting formation of a host–guest inclusion complex (Fig. 1). The inner cavity of β-CD, a hydrophobic environment, can act in several ways. On one hand, it may promote the dual fluorescence emission behaviour by facilitating proton transfer along the C(4)═O···HO—(3)C co-ordinate due to the absence of hydrogen bonding perturbations of bulk water. On the other hand, it can also protect the fluorophoric moiety from excited-state deactivation caused by internal conversion and collisions with the water molecules from the bulk solution, thus producing an increase in fluorescence intensity.

Interestingly, upon addition of 10 mM β-CD the normal peak shifts from 475 to 460 nm while the tautomer peak shifts from 533 to 542 nm. This feature of the dual emission, i.e., increasing separation of the two peaks upon gradual addition of β-CD, was also previously reported for other related flavonoids (Banerjee, Basu, & Sengupta, 2007). In addition to being continuously shifted to lower wavelengths, the peak for normal myricetin also broadens up. Changes in the normal fluorescence behaviour upon inclusion suggest a large change of the transition dipole moment between the ground (S0) and first excited state (S1) of myricetin.

It is well documented that in rigid media the dipolar reorientation of the solvent cage around the excited fluorophore gets inhibited, resulting in blue shifts of the fluorescence band due to emission from the unrelaxed Franck–Condon excited state. We also envisage emission from the unrelaxed Franck–Condon excited state in case of nano-encaged myricetin within β-CD. Since excited-state relaxation is highly restricted within the nano-cavity, emission occurs from several unrelaxed Franck–Condon states which explain the observed continuous broadening of the peak profile along with its concomitant shift to higher energy upon progressive inclusion within the β-CD cavity.

The presence of β-CD also causes pronounced blue shifts of the excitation maxima of myricetin from those found in aqueous media. Such blue shifts indicate conspicuous changes in the microenvironment of the myricetin on entrapment inside the β-CD cavity. Interestingly, the excitation profile monitored in the blue-violet emission region shows a more significant blue shift than that of the green tautomer emission (Fig. 1S). This indicates that the two emission bands originate from two distinct ground state populations differing in their microenvironments.

3.2. Determination of binding constant

The equilibrium constant (K) for binding of myricetin with β-CD was determined by monitoring the fluorescence intensity of myricetin in presence of increasing concentrations of β-CD. For a 1:1 complex formation between a fluorescent guest molecule and β-CD the binding constant can be calculated using a modified Benesi–Hildebrand equation (Guzzo et al., 2006):

$$1/\Delta F = 1/(\Delta F_{max} K[\beta - CD]) + 1/\Delta F_{max} \quad (5)$$

where $\Delta F = F_x - F_0$, F_x and F_0 represent the fluorescence intensities of myricetin in the presence and absence of added β-CD, respectively, ΔF_{max} is the maximum change in fluorescence intensity and K is the binding constant for the 1:1 complex.

A plot of $1/\Delta F$ vs. 1/[β-CD] shown in Fig. 2A exhibits strong linearity and indicates formation of inclusion complex between the host (β-CD) and the guest (myricetin) with a stoichiometry of 1:1. The equilibrium constant (K) for the myricetin–β-CD complex obtained by fitting the fluorescence data of Fig. 2A to Eq. (5) was found to be $439 \pm 18\,M^{-1}$ at 25 °C. This value is comparable to the observed binding constant of 3-hydroxyl flavone (simplest structural analogue of flavonoids) with β-CD at 25 °C ($K = 498.21\,M^{-1}$) (Banerjee & Sengupta, 2006) and stability constant (K_s) of myricetin–β-CD complex ($398.92\,M^{-1}$) using phase-solubility study (Kwon et al., 2010).

3.3. Thermodynamic parameters involved in the inclusion complex formation

Thermodynamic parameters such as enthalpy change (ΔH^0), entropy change (ΔS^0) and free energy change (ΔG^0) of the complexation reaction were evaluated from the van't Hoff plot of $\ln K$ versus $1/T$ (Fig. 2B), obtained using values of the equilibrium constant K determined at three different temperatures (298, 303,

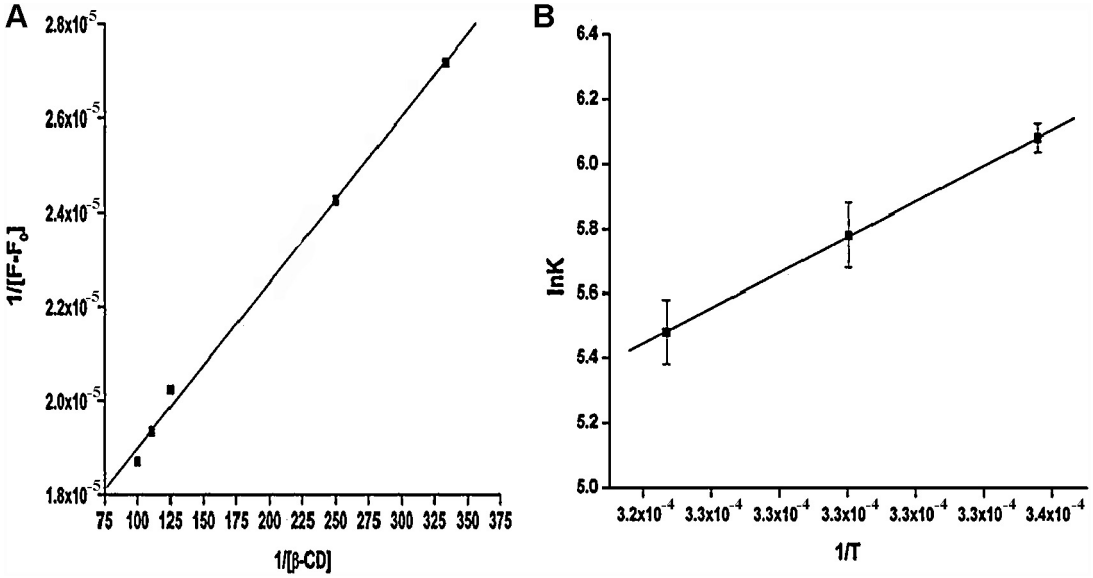

Fig. 2. (A) Double reciprocal plot of myricetin interaction with β-CD at 25 °C. (B) Temperature dependence of binding constant (van't Hoff plot). Each data point indicates the average of three independent determinations and error bars indicate the standard deviation of the three measurements.

and 308 K). Fitting the data of Fig. 2B to Eq. (6) yielded values of $-\Delta H^0$ and ΔS^0, from which ΔG^0 was calculated using Eq. (7):

$$\ln K = -\frac{\Delta H^0}{RT} + \frac{\Delta S^0}{R} \quad (6)$$

$$\Delta G^0 = \Delta H^0 - T\,\Delta S^0 \quad (7)$$

where R is the gas constant and T the absolute temperature. Values of the thermodynamic parameters so calculated are listed in Table 1. Table 1 reveals that complexation of myricetin with β-CD in aqueous solution is accompanied by a negative ΔG^0 and negative ΔH^0, reflecting a spontaneous, exothermic process. Large negative enthalpy (ΔH^0) changes are usually attributed to strong van der Waals interactions due to strong size and shape complementarities as well as formation of hydrogen bonds between myricetin and β-CD. Strong spatial fit of myricetin within β-CD cavity results in release of enthalpy-rich water molecules from the β-CD cavity.

The standard entropy change (ΔS^0) is also negative, corresponding to a decrease in the rotational and translational degrees of freedom upon inclusion of the guest into the nanocavity of β-CD. Generally, two opposing effects contribute to the total entropy changes during host–guest complex formation. Loss of rotational and translational degrees of freedom of free host and guest upon complex formation decreases the entropy, while appropriate fitting of the guest within host cavity results in dehydration of the guest and release of ordered water molecules surrounding the guest increases the entropy of the solution. These two effects nearly cancel out each other, resulting in very small entropy value. But the negative value indicates that the first phenomenon is slightly more pronounced than the other for myricetin–β-CD inclusion complex formation.

Table 1
Thermodynamic parameters of inclusion complexes between β-CD and myricetin at 25 °C.

Thermodynamic parameter	Value (from Fig. 2B)
ΔH^0	$-(10.93 \pm 0.02)$ kcal/mol
ΔS^0	$-(0.0246 \pm 0.00007)$ kcal mol^{-1} K^{-1}
ΔG^0	−3.60 kcal/mol

3.4. Fluorescence anisotropy

Fluorescence anisotropy (r) is a useful parameter to assess the rigidity of the local environment of the fluorophore. A low anisotropy value, usually found in aqueous solution, indicates high degree of rotational freedom while high anisotropy values point to motionally constrained environments. Typical fluorescence anisotropy data collected at the ESIPT tautomer emission band of myricetin (λ_{em} = 540 nm) with increasing β-CD concentration are shown in Fig. 3A. The progressive increase in anisotropy with increasing concentration of β-CD confirms that more and more myricetin become confined in the motionally restricted nanocavity of β-CD.

3.5. Induced CD (ICD) spectra

Myricetin being an inherently achiral molecule does not display any circular dichroism signal in aqueous solution. Interestingly, a positive Cotton effect appears when β-CD is added to the solution, as shown in Fig. 3B. The shape and intensity of the induced CD band reveal the adopted orientation of the guest molecules when inserted into the host. A positive signal indicates incorporation of myricetin inside β-CD where the electric dipole moment vector of myricetin coincides with the β-CD symmetry axis (Szejtli, 1988). The position of the ICD band coincides with Band II, which is attributed to absorption of the benzoyl moiety (A + C ring) and is essentially π–π^* in nature (Zeng et al., 2003). The observation of the ICD signal in this wavelength region, corresponding to the electronic transitions, is further indication that myricetin experiences strong interaction with the toroidal framework of the β-CD nanocavity through its benzoyl moiety.

3.6. Time-resolved fluorescence

Time-resolved fluorescence studies were performed to understand how encapsulation within the β-CD nanocavity influences the stability and dynamics of the excited states of normal and ESIPT tautomer emission of myricetin. Table 2 summarises the results of analysis of the fluorescence total intensity decay profiles for normal (λ_{ex} = 370 nm, λ_{em} = 470 nm) and tautomeric form of myricetin

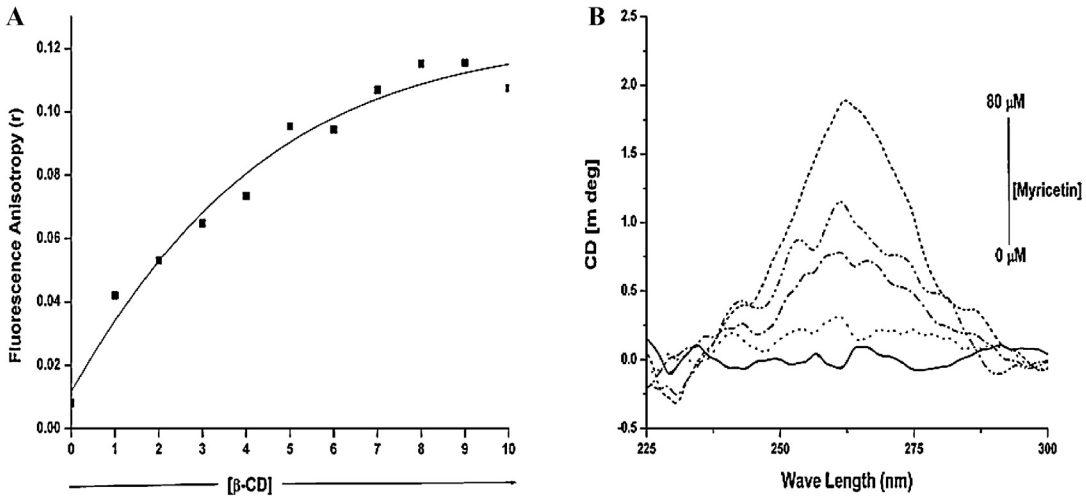

Fig. 3. (A) Variation of fluorescence anisotropy (r) of myricetin with increasing concentration of β-CD (λ_{ex} = 370 nm, λ_{em} = 540 nm). (B) Induced circular dichroism (ICD) spectra of myricetin upon incorporation into β-CD.

(λ_{ex} = 370 nm, λ_{em} = 540 nm) in different solvents and in presence of varying concentrations of β-CD.

The fluorescence intensity decay profile of normal myricetin was satisfactorily deconvoluted into a sum of three exponential decays, as indicated by the corresponding χ^2 value. In ethanol, the predominant (58%) decay component had a lifetime of 2.4 ns, while a significant contribution (32%) was observed from a species with a long lifetime of 9.1 ns. In addition, a minor contribution from a short lifetime (0.28 ns) species was also detected. The situation is markedly different in aqueous medium, where the principal component (∼91.6%) is a very short-lived species (with lifetime of 15 ps) whereas the two long lifetime species (with lifetimes of 1.0 and 6.6 ns) have negligible contributions. This result can be attributed to the high solvent polarity of water, in which the lifetime of myricetin decreases due to fast deactivation processes mediated through freely rotating water dipoles. The tri-exponential decay pattern can be rationalised in terms of differently solvated species in these solvents. The situation changes in presence of β-CD, where the time-resolved fluorescence intensity of nano-encaged myricetin fits to a biexponential decay profile with a major picosecond component and a minor nanosecond component. These sharp changes in the lifetime behaviour reflect a drastic change in the microenvironment upon encapsulation. The long lifetime component could presumably arise from differently solvated or hydrogen bonded species of nano-encaged myricetin molecules. It is to be noted that the mean lifetime ($\langle\tau\rangle$) gradually decreases with increasing β-CD concentration from 1 to 10 mM. The lifetime data suggest a mechanism of peak broadening and blue shift observed for the 'normal' steady-state fluorescence emission of myricetin inside β-CD. Since the major contribution to the time-resolved decay of the 'normal' species within β-CD comes from a very short lifetime species, entrapment in the nano-cavity will prevent it from undergoing excited state relaxation. Moreover, the rigid β-CD cavity will inhibit the dipolar reorientation of the solvent cage around the excited fluorophore. Thus fluorescence might occur from many unrelaxed Frank–Condon excited vibronic states, leading to blue shift and concomitant broadening of the emission peak when compared to water. The predominance of the picosecond component in the fluorescence decay of myricetin in water and inside the β-CD nanocavity reflects the comparable nature of its microenvironments in these two media. It indicates that the fluorophoric moiety is probably placed near the hydroxyl rim of β-CD, making it solvent exposed. The fluorophore may also experience hydrogen bonding interactions with the OH groups of β-CD, which will shorten the lifetime by facilitating the deactivation process.

The fluorescence decay profile of myricetin tautomer in aqueous solution could be fitted by the sum of two exponential decays, as indicated by the corresponding χ^2 value. The predominant contribution (89%) came from a sub-nanosecond component with lifetime of 0.11 ns, while a minor contribution (11%) came from a species with lifetime of 1.6 ns. In hydrogen bond donor–acceptor solvents like ethanol, fitting the decay profile yielded three lifetimes, of which two were in the nanosecond (11.4 ns and 3.1 ns) and one in the sub-nanosecond range (0.47 ns). It is noteworthy that the lifetimes of both the short- and the long-lived species increased upon decreasing the solvent polarity. In presence of β-CD, a major contribution comes from sub-nanosecond tautomeric lifetime species in addition to a minor nanosecond component. The major picosecond lifetime species observed in presence of 1 mM β-CD can be attributed to un-complexed myricetin due to the

Table 2
Fluorescence total intensity decay parameters of myricetin emission in different solvents and in presence of varying concentrations of β-CD.

Medium	Species	α_1 (%)	τ_1 (ns)	α_2 (%)	τ_2 (ns)	α_3 (%)	τ_3 (ns)	$\langle\tau\rangle$[a] (ns)	χ^2	DW parameter
Water	Normal	5.37	6.6	3.02	1.0	91.61	0.015	5.95	1.03	1.05
	Tautomer	10.66	1.6	–	–	89.34	0.11	1.06	1.06	0.66
Ethanol	Normal	32.06	9.1	58.24	2.4	9.70	0.28	6.89	1.16	1.74
	Tautomer	12.23	11.4	26.13	3.1	61.65	0.47	7.43	1.22	1.9
1 mM β-CD	Normal	22.6	4.80	–	–	77.4	0.036	4.68	1.04	0.78
	Tautomer	6.49	3.9	34.25	0.36	59.25	0.07	2.48	1.08	0.93
10 mM β-CD	Normal	23.19	3.53	–	–	76.81	0.063	3.36	1.00	0.64
	Tautomer	10.78	2.98	–	–	89.22	.228	1.91	1.04	0.84

[a] $\langle\tau\rangle = (\alpha_1\tau_1^2 + \alpha_2\tau_2^2 + \alpha_3\tau_3^2)/(\alpha_1\tau_1 + \alpha_2\tau_2 + \alpha_3\tau_3)$.

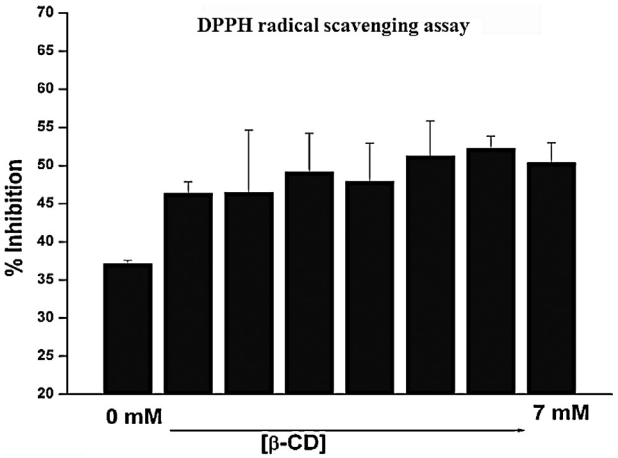

Fig. 4. Percentage inhibition of DPPH radical by myricetin and myricetin with increasing concentrations of β-CD. Each data point indicates the average of three independent determinations and error bars indicate the standard deviation of the three measurements.

similarity of its lifetime to the lifetime of the short-lived species in water. It is to be noted that the mean lifetime ($\langle\tau\rangle$) increases in presence β-CD, compared to that in aqueous media, signifying encapsulation of the fluorophore in relatively less polar environment than water. But the lifetime is significantly smaller than in ethanolic media, indicating that the fluorophore is not deeply embedded inside the cavity, where the polarity would be comparable to that of ethanol (Frankewich, Thimmaiah, & Hinze, 1991). It thus appears that the fluorophoric moiety of myricetin partitions itself near the hydroxyl rim of β-CD, where the polarity of the microenvironment is similar to that of water–ethanol mixture. The hydrogen bonding perturbation induced by the hydroxyl rim of β-CD also can contribute to the observed lifetime shortening of nano-encaged myricetin.

3.7. Anti-oxidant activity analysis of encapsulated myricetin

The bleaching of DPPH radical absorbance with an antioxidant reflects the latter's ability to scavenge the radical. The quenching of DPPH radical absorbance by myricetin in the free and encapsulated forms is shown in Fig. 4 and expressed in percentage inhibition.

The data show that 1 μM myricetin in aqueous solution can scavenge 37% of DPPH radical. The scavenging ability increases to 47% in presence of 1 mM β-CD and can go up to 52% with increasing β-CD concentration up to 7 mM for the same concentration of myricetin. That the % inhibition does not change very much beyond ~1 mM added β-CD is due to the fact that for the concentration of myricetin (1 μM) used in these measurements, the complexation reaction (at 1:1 stoichiometry) is almost complete at 1 mM concentration of β-CD. Since, the enhancement of the radical scavenging activity of encapsulated myricetin saturates at 1 mM β-CD concentration, we performed Student's *t*-test to understand the statistical significance of the observed data. Calculated *p* value at 99% level of significance with respect to the control experiment (antioxidant activity of only myricetin) is 0.0043. Thus the observed effect of increasing antioxidant activity upon encapsulation is statistically very significant. This result clearly indicates that inclusion in β-CD nanocavity influences myricetin in such a way that it can more efficiently scavenge radicals. β-CD itself has no effect on the antioxidant activity; in fact, high concentrations of it produce a little pro-oxidant effect (data not shown). In order to explore whether the inclusion has an influence on the antioxidant capacity of myricetin, a fixed concentration of the myricetin (1 μM) was used in assaying all the sets. This confirms that the antioxidant ability of myricetin increases in encapsulated form. These results are in agreement with those of Stražišar, Andrenšek, and Šmidovnik (2008), who showed that o- and m-coumaric acid upon inclusion within β-CD cavity possess significantly higher antioxidant activity. Recently, Jullian, Moyano, Yanez, and Olea-Azar (2007) also found that quercetin–cyclodextrin inclusion complexes showed a higher radical scavenging capability compared to quercetin in free form.

3.8. Molecular docking

In order to rationalise our experimental data and to infer the mode of inclusion, we have performed molecular docking analysis of myricetin with β-CD using AutoDock. The lowest energy docked conformation, shown in Fig. 5, reveals that myricetin forms inclusion complex with β-CD and its A-ring is clearly dipped inside the β-CD cavity, close to the primary hydroxyl rim of the β-CD cavity. Analysis of host–guest interaction energies as obtained from docking studies also reveal that hydrogen bonding and van der Waals interactions are the predominant forces of complexation.

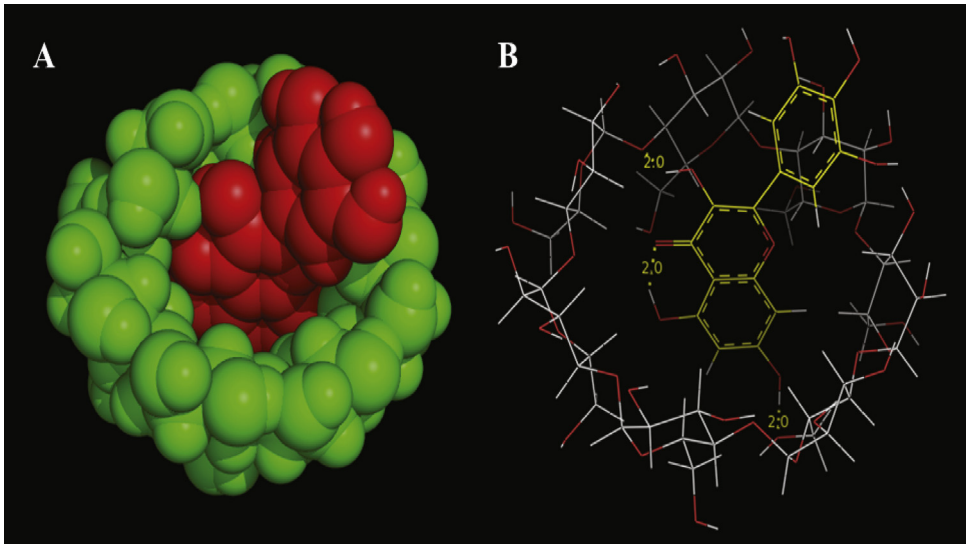

Fig. 5. Lowest energy myricetin–β-CD docked complex. (A) CPK model representation of the complex; green represents β-CD and red colour represents myricetin. (B) Stick representation; yellow stick represents myricetin and β-CD coloured as white and red sticks.

Table 3
Calculated energy values and dipole moment of myricetin and β-CD and the corresponding changes in energy and dipole moment upon inclusion.

Methods used	Parameter	Myricetin	β-CD	β-CD–myricetin complex (phenyl inclusion) 1:1	β-CD–myricetin complex (chromone inclusion) 1:1 (kcal/mol)
PM3	Energy, E (kcal/mol)	−3829.99	−14,368.24	−18,202.97	−18,207.62
	[a] ΔE (kcal/mol)	–	–	−4.74	−9.39
	Dipole moment (Debye)	4.38	5.62	5.81	5.44
	[b] ΔDipole moment (Debye)	–	–	−4.19	−4.56
B3LYP/3-21G* (PCM water model)	Energy, E (kcal/mol)	−735,613.30	−2,666,553.05	−3,402,169.87	−3,402,208.28
	[a] ΔE (kcal/mol)	–	–	−3.52	−41.93
	Dipole moment (Debye)	7.50	10.38	12.65	11.67
	[b] ΔDipole moment (Debye)	–	–	−5.23	−6.21
B3LYP/6-31G (PCM water model)	Energy, E (kcal/mol)	−739,479.21	−2,680,455.25	−3,419,924.12	−3,419,952.20
	[a] ΔE (kcal/mol)	–	–	10.34	−17.74
	Dipole moment (Debye)	8.04	10.24	13.11	10.88
	[b] ΔDipole moment (Debye)	–	–	−5.17	−7.40

[a] $\Delta E = E_{complex} - (E_{myricetin} + E_{\beta\text{-CD}})$.
[b] ΔDipole moment = Dipole moment$_{complex}$ − (Dipole moment$_{myricetin}$ + Dipole moment$_{\beta\text{-CD}}$).

As evident from Fig. 5A, in this inclusion mode myricetin binds to the cavity of β-CD that allows maximum surface complementarities between the host and the guest ligand. AutoDock also predicts that myricetin is involved in four hydrogen bonding interactions with the primary and secondary hydroxyl group and also with the glycosidic oxygen of β-CD (Fig. 5B). It is to be noted that the binding forces for the complexation predicted by docking is in accordance with the results obtained from thermodynamic analysis of binding constant. The lowest energy structure also reveals that myricetin is included through the A-ring along the molecular axis of β-CD with a slight tilt that allows maximum hydrogen bonding interaction between the host and the guest. This mode of inclusion also explains the observed ICD band in the benzoyl moiety (A + C) ring of myricetin upon inclusion. It is to be noted that the intra-molecular hydrogen bonding, in between C(3)—OH and C(4)═O group, of myricetin that is responsible of the ESIPT process is preserved in the β-CD cavity.

By analysing all the 250 possible docked conformation of myricetin with β-CD, we observed two possible modes of inclusion of myricetin into β-CD cavity: (A) through A-ring (chromone moiety) and (B) through B-ring (phenyl ring), shown in Fig. 2S.

To further ascertain the preferred mode of inclusion of myricetin within β-CD, we have performed cluster analysis with all the 250 docked complexes using a cut-off of 2 Å RMSD and by using a probability score, p, introduced previously by Sotriffer, Winger, Liedl, Rode, and Varga (1996). This parameter systematically describes how well the predicted structures behave statistically and energetically by using the combination of the occurring frequency (H_n) and the corresponding interaction energy (E_n) as follows:

$$p = \frac{H_n}{N} \exp - \frac{E_n - E_1}{0.594} \quad (8)$$

where H_n refers to the total number of conformations in which myricetin adopted similar orientations in molecular docking runs and N the total number of runs, i.e., 250 in our case, E_n is the interaction energy of the nth predicted model and E_1 is the lowest interaction energy that appears in the docking runs. 0.594 comes from the gas constant multiplied by room temperature (i.e., 0.594 kcal/mol). The highest score corresponds to the most favourable model. Results are summarised in Table 1S.

Table 1S indicates that the structure of the inclusion complex in which the A-ring of myricetin is dipped into the β-CD cavity is energetically and statistically favoured over the other mode of inclusion, as is evident from the p value and other related energy parameters.

3.9. Conformational analysis of the inclusion process using QM calculation

To obtain a more detailed energetic description of the process of inclusion, we employed quantum mechanical calculations with more accurate nuclear and electronic energy terms describing the system while taking account of β-CD flexibility and solvation effect through implicit solvent model. The energy change accompanying the formation of the 1:1 complex for two different modes of myricetin inclusion within β-CD, identified in the docking study, can be calculated as:

$$\Delta E = E_{complex} - (E_{myricetin} + E_{\beta\text{-CD}}) \quad (9)$$

where $E_{complex}$, $E_{myricetin}$, and $E_{\beta\text{-CD}}$ are the energies of the complex, free myricetin (guest) and free β-CD (host), respectively. Detailed energetic descriptions for two possible modes of inclusion complex formation are summarised in Table 3.

To ensure that the observed result is independent of the applied basis set, we carried out energy calculations with two different basis sets, 3-21G* and 6-31G. The large size of the inclusion complex limits the use of higher basis sets. So we first chose a moderate basis set where we took account of d-orbital polarisation and in the next one we used a relatively higher basis set with no polarisation. We also considered the effect of solvation on the inclusion process by considering implicit solvent effect by PCM model. Comparison of the calculations of different QM methods reveals that the inclusion of myricetin within β-CD through the chromone ring is clearly favourable over the other mode of inclusion. Even using the B3LYP/6-31G basis set, inclusion through phenyl ring is energetically unfavourable. An interesting observation is the change of dipole moment due to complexation. QM calculation predicts that strong dipolar relaxation occurs when myricetin is included through chromone ring within β-CD nanocavity. Thus dipole–dipole interaction is one of the driving quantum chemical parameter that dictates the mode of inclusion during complexation.

3.10. Theoretical insight on the anti-oxidant property of encapsulated myricetin

Since the most probable mode of inclusion is found to be through the chromone ring, we further calculated the different quantum chemical parameters of encapsulated myricetin on the basis of that inclusion mode to understand the origin of enhanced antioxidant potential of encapsulated myricetin. The electron-giving ability of the antioxidants correlates very well with the energy level of the

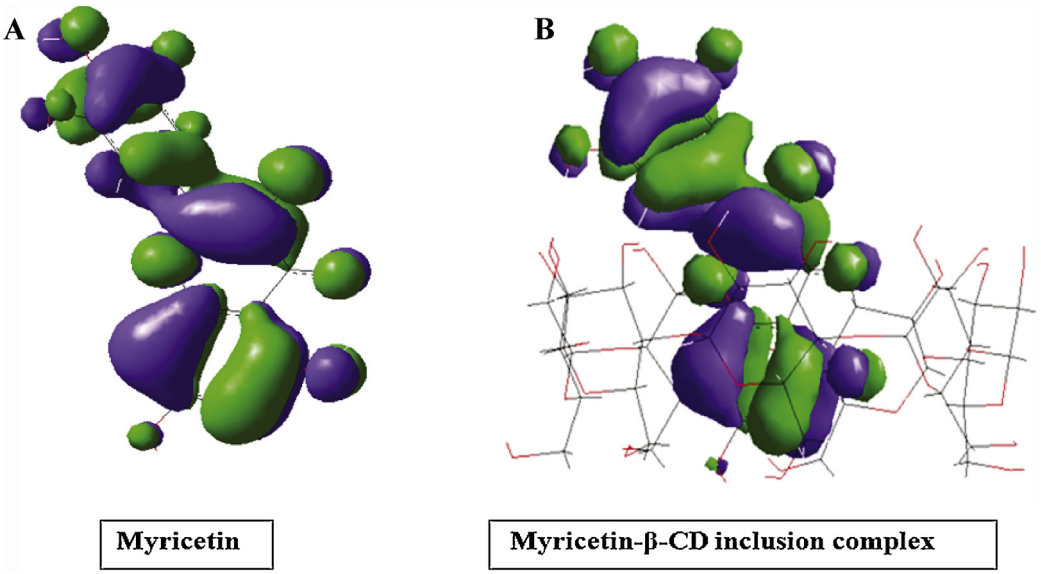

Fig. 6. Distribution of highest occupied molecular orbital (HOMO) of free myricetin (A) and myricetin nano-encapsulated within β-CD (B). The orbitals have been plotted on the myricetin skeleton in isosurface rendering mode with two colours (green and purple), which represent the positive and negative isosurfaces, respectively. β-CD has been rendered in the stick model in (B).

highest occupied molecular orbital (E_{HOMO}) and the relative adiabatic ionisation potential (IP). Table 2S lists the HOMO and LUMO energies of myricetin and nano-encapsulated myricetin obtained by using different QM methods.

It is quite evident from Table 2S that E_{HOMO} increases when myricetin is encapsulated within β-CD nano-cavity. According to Koopmans' theorem (Leach, 1996),

$$\text{IP (Ionisation Potential)} = -E_{HOMO} \quad (10)$$

IP value decreases after formation of inclusion complex. Thus the electron donating ability of myricetin in the encapsulated form enhances, reflecting the enhanced antioxidant potential of nano-encapsulated myricetin observed by DPPH radical scavenging assay (Fig. 4).

Fig. 6 clearly demonstrates that HOMO is localised over the entire myricetin molecule. The β-CD cavity reduces the delocalisation of HOMO electron density, specifically on the 7-OH part of the A-ring of myricetin, resulting in an enhancement of the E_{HOMO}. Encapsulation within β-CD also decreases the E_{LUMO}, thus reducing the HOMO–LUMO energy gap, an important determinant of antioxidant potential. Lowering this energy gap can enhance the antioxidant potential, as shown by Rackova et al. for polyphenols (Rackova et al., 2005). It is well characterised that the radical formation site for poly-hydroxyl flavonol is on the B-ring (Trouillas, Marsal, Siri, Lazzaroni, & Duroux, 2006). Specifically, the 4′-OH is the most preferred site for hydrogen abstraction leading to the formation of 4′-radical due to the formation of para-quinonoid structure (Trouillas et al., 2006). Interestingly, we found that the inclusion complex formation for myricetin radical with β-CD is more favoured compared to the neutral myricetin by 0.26 eV (data not shown). This observation can be rationalised by the fact that formation of myricetin radical further facilitates the formation of more stable inclusion complex.

We have further analysed the effect of nano-encapsulation on other higher energy unoccupied orbital. Upon inclusion, the electronic states of myricetin undergo significant changes. DFT calculations by using two different basis sets reveal that HOMO energy increases upon inclusion within the β-CD cavity while, on the contrary, energies of the unoccupied orbitals (e.g. LUMO, LUMO-1, LUMO-2) decrease upon inclusion (Fig. 3S).

4. Conclusion

By using steady-state and time-resolved fluorescence spectroscopy in combination with induced circular dichroism spectroscopy, molecular modelling and quantum chemical calculations we have explored the structural and energetic aspects of nano-encapsulation of myricetin within β-CD cavity. The calculated equilibrium constant for myricetin–β-CD inclusion complex is $439 \pm 18\ M^{-1}$ at 25 °C for 1:1 stoichiometry. Calculation of thermodynamic parameters indicates that the inclusion of myricetin within β-CD cavity is a spontaneous, exothermic process and strong van der Waals as well as hydrogen bonding interactions are found to be the driving forces for complexation. The standard entropy changes (ΔS^0) are also negative, corresponding to a decrease in the rotational and translational degrees of freedom upon the inclusion of the guest into β-CD. Interestingly, we observed that the mean excited state lifetime ($\langle\tau\rangle$) of normal form of myricetin decreases upon increasing β-CD concentration and the principal contribution to the fluorescence decay of the normal fluorophore within the β-CD cavity comes from a very short-lived species. β-CD nano-cavity prevents relaxation of excited state of the fluorophore which has been attributed to emission from many unrelaxed Frank–Condon excited vibronic states, leading to blue shift and concomitant broadening of the emission peak.

CD spectroscopy along with docking study reveals that the possible mode of inclusion of myricetin within the β-CD nanocavity is through its benzoyl moiety (A + C ring). Quantum chemical calculations confirm that the inclusion complex in which the A-ring of myricetin is dipped into the β-CD cavity is energetically and statistically favoured over the other mode of inclusion. Using the DPPH radical scavenging assay we observed that myricetin in the encapsulated form is a much stronger antioxidant than in its free form. Quantum mechanical studies predict the HOMO of β-CD encapsulated myricetin to be less delocalised than free myricetin. This destabilisation of HOMO increases HOMO energy and decreases the ionisation potential. In addition, encapsulation within β-CD decreases the energy of the lowest unoccupied molecular orbital (LUMO), thus reducing the HOMO–LUMO energy gap. These observations rationalise the enhancement of antioxidant potential of nano-caged myricetin.

Our study provides a detailed structural description of myricetin upon nano-encapsulation into β-CD cavity, enabling an insight of the observed enhancement of the bioactive properties of myricetin upon inclusion. This study also provides a pipeline for designing suitable CDx derivatives that can further improve the activity of myricetin by extending its application as a therapeutic agent as well as functional food. The present findings open up new genera of research interests in cyclodextrin chemistry, wherein CDx are used to improve the bioactive properties of the encapsulated guests along with concomitant improvement in pharmacokinetic aspects.

Appendix A. Supplementary data

Supplementary data associated with this article can be found, in the online version, at http://dx.doi.org/10.1016/j.carbpol.2013.08.008.

References

Banerjee, A., Basu, K., & Sengupta, P. K. (2007). Effect of β-cyclodextrin nanocavity confinement on the photophysics of robinetin. *Journal of Photochemistry and Photobiology B: Biology*, *89*, 88–97.

Banerjee, A., & Sengupta, P. K. (2006). Encapsulation of 3-hydroxyflavone and fisetin in β-cyclodextrins: Excited state proton transfer fluorescence and molecular mechanics studies. *Chemical Physics Letters*, *424*, 379–386.

Burits, M., & Bucar, F. (2000). Antioxidant activity of *Nigella sativa* essential oil. *Phytotherapy Research*, *14*, 323–328.

Chakraborty, S., Basu, S., Lahiri, A., & Basak, S. (2010). Inclusion of chrysin in β-cyclodextrin nanocavity and its effect on antioxidant potential of chrysin: A spectroscopic and molecular modeling approach. *Journal of Molecular Structure*, *977*, 180–188.

Chakraborty, S., Kumar, S., & Basu, S. (2011). Conformational transition in the substrate binding domain of β-secretase exploited by NMA and its implication in inhibitor recognition: BACE1–myricetin a case study. *Neurochemistry International*, *58*, 914–923.

Chaudhuri, S., Chakraborty, S., & Sengupta, P. K. (2010). Encapsulation of serotonin in β-cyclodextrin nano-cavities: Fluorescence spectroscopic and molecular modeling studies. *Journal of Molecular Structure*, *975*, 160–165.

Formica, J. V., & Regelson, W. (1995). Review of the biology of quercetin and related bioflavonoids. *Food and Chemical Toxicology*, *33*, 1061–1080.

Frankewich, R. P., Thimmaiah, K. N., & Hinze, W. L. (1991). Evaluation of the relative effectiveness of different water-soluble beta-cyclodextrin media to function as fluorescence enhancement agents. *Analytical Chemistry*, *63*, 2924–2933.

Groot, H. D., & Rauen, U. (1998). Tissue injury by reactive oxygen species and the protective effects of flavonoids. *Fundamental & Clinical Pharmacology*, *12*, 249–255.

Guzzo, M. R., Uemi, M., Donate, P. M., Nikolaou, S., Machado, A. E. H., & Okano, L. T. (2006). Study of the complexation of fisetin with cyclodextrins. *The Journal of Physical Chemistry A*, *110*, 10545–10551.

Hyperchem. (2002). *Hypercube, Inc., USA*.

Jullian, C., Moyano, L., Yanez, C., & Olea-Azar, C. (2007). Complexation of quercetin with three kinds of cyclodextrins: An antioxidant study. *Spectrochimica Acta Part A: Molecular and Biomolecular Spectroscopy*, *67*, 230–234.

Ko, C. H., Shen, S. C., Lee, T. J., & Chen, Y. C. (2005). Myricetin inhibits matrix metalloproteinase 2 protein expression and enzyme activity in colorectal carcinoma cells. *Molecular Cancer Therapeutics*, *4*, 281–290.

Kusumoto, Y. (1987). A spectrofluorimetric method for determining the association constants of pyrene with cyclodextrins based on polarity variation. *Chemical Physics Letter*, *136*, 535–538.

Kwon, Y., Kim, H., Park, S., & Jung, S. (2010). Enhancement of solubility and antioxidant activity of some flavonoids based on the inclusion complexation with sulfobutylether β-cyclodextrin. *Bulletin of Korean Chemical Society*, *31*, 3035–3037.

Lakowicz, J. R. (1999). *Principles of fluorescence spectroscopy* (2nd ed.). New York: Plenum.

Lamson, D. W., & Brignall, M. S. (2000). Antioxidants and cancer III: Quercetin. *Alternative Medical Review*, *5*, 196–208.

Leach, A. R. (1996). Quantum mechanical models. In *Molecular modelling: Principles and applications*. London: Longman publishing.

Loftsson, T., Másson, M., & Sigurdsson, H. H. (2002). Cyclodextrins and drug permeability through semi-permeable cellophane membranes. *International Journal of Pharmaceutics*, *232*, 35–43.

Lucas-Abellán, C., Fortea, I., Gabaldón, J. A., & Núñez-Delicado, E. (2007). Encapsulation of quercetin and myricetin in cyclodextrins at acidic pH. *Journal of Agricultural and Food Chemistry*, *56*, 255–259.

Meijer, D. K., & van der Sluijs, P. (1989). Covalent and noncovalent protein binding of drugs: Implications for hepatic clearance, storage, and cell-specific drug delivery. *Pharmaceutical Research*, *6*(2), 105–118.

Middleton, E. J. (1998). Effect of plant flavonoids on immune and inflammatory cell function. *Advances in Experimental Medicine and Biology*, *439*, 175–182.

Miyake, K., Arima, H., Hirayama, F., Yamamoto, M., Horikawa, T., Sumiyoshi, H., et al. (2000). Improvement of solubility and oral bioavailability of rutin by complexation with 2-hydroxypropyl-β-cyclodextrin. *Pharmaceutical Development and Technology*, *5*, 399–407.

Morris, G. M., Goodsell, D. S., Halliday, R. S., Huey, R., Hart, W. E., Belew, R. K., et al. (1998). Automated docking using a Lamarckian genetic algorithm and an empirical binding free energy function. *Journal of Computational Chemistry*, *19*, 1639–1662.

Ong, K. C., & Khoo, H. E. (1997). Biological effects of myricetin. *General Pharmacology: The Vascular System*, *29*, 121–126.

Ono, K., Yoshiike, Y., Takashima, A., Hasegawa, K., Naiki, H., & Yamada, M. (2003). Potent anti-amyloidogenic and fibril-destabilizing effects of polyphenols in vitro: Implications for the prevention and therapeutics of Alzheimer's disease. *Journal of Neurochemistry*, *87*, 172–181.

Paul, B. K., & Guchhait, N. (2010). Modulated photophysics of an ESIPT probe 1-hydroxy-2-naphthaldehyde within motionally restricted environments of liposome membranes having varying surface charges. *The Journal of Physical Chemistry B*, *114*, 12528–12540.

Rackova, L., Firakova, S., Kostalova, D., Stefek, M., Sturdik, E., & Majekova, M. (2005). Oxidation of liposomal membrane suppressed by flavonoids: Quantitative structure–activity relationship. *Bioorganic & Medicinal Chemistry*, *13*, 6477–6484.

Rasheed, A., Kumar, A. C. K., & Sravanthi, V. V. N. S. S. (2008). Cyclodextrins as drug carrier molecule: A review. *Scientia Pharmaceutica*, *76*, 567–598.

Rusa, C. C., Luca, C., & Tonelli, A. E. (2001). Polymer–cyclodextrin inclusion compounds: Toward new aspects of their inclusion mechanism. *Macromolecules*, *34*, 1318–1322.

Schmidt, M. W., Baldridge, K. K., Boatz, J. A., Elbert, S. T., Gordon, M. S., Jensen, J. H., et al. (1993). General atomic and molecular electronic structure system. *Journal of Computational Chemistry*, *14*, 1347–1363.

Sengupta, P. K., & Kasha, M. (1979). Excited state proton-transfer spectroscopy of 3-hydroxyflavone and quercetin. *Chemical Physics Letter*, *68*, 382–385.

Shimmyo, Y., Kihara, T., Akaike, A., Niidome, T., & Sugimoto, H. (2008). Flavonols and flavones as BACE-1 inhibitors: Structure–activity relationship in cell-free, cell-based and in silico studies reveal novel pharmacophore features. *Biochimica et Biophysica Acta (BBA): General Subjects*, *1780*(5), 819–825.

Sotriffer, C. A., Winger, R. H., Liedl, K. R., Rode, B. M., & Varga, J. M. (1996). Comparative docking studies on ligand binding to the multispecific antibodies IgE-La2 and IgE-Lb4. *Journal of Computer-Aided Molecular Design*, *10*, 305–320.

Soujanya, T., Krishna, T. S. R., & Samanta, A. (1992). Effect of β-cyclodextrin on intramolecular charge-transfer emission of 4-aminophthalimide. *Journal of Photochemistry and Photobiology A: Chemistry*, *66*, 185–192.

Stražišar, M., Andrenšek, S., & Šmidovnik, A. (2008). Effect of β-cyclodextrin on antioxidant activity of coumaric acids. *Food Chemistry*, *110*, 636–642.

Szejtli, J. (1988). *Cyclodextrin technology*. Chicago: Kluwer Academic Publishing.

Szejtli, J. (2004). Past, present and future of cyclodextrin research. *Pure and Applied Chemistry*, *76*, 1825–1845.

Trouillas, P., Marsal, P., Siri, D., Lazzaroni, R., & Duroux, J. L. (2006). A DFT study of the reactivity of OH groups in quercetin and taxifolin antioxidants: The specificity of the 3-OH site. *Food Chemistry*, *97*, 679–688.

Xu, H., Ziegelin, G., Schröder, W., Frank, J., Ayora, S., Alonso, J. C., et al. (2001). Flavones inhibit the hexameric replicative helicase RepA. *Nucleic Acids Research*, *29*, 5058–5066.

Zeng, Y. B., Yang, N., Liu, W. S., & Tang, N. (2003). Synthesis, characterization and DNA-binding properties of La(III) complex of chrysin. *Journal of Inorganic Biochemistry*, *97*, 258–264.